

# Transfer Printing of Semiconductor Nanowire Lasers

A. Hurtado<sup>1\*</sup>, D. Jevtics<sup>1</sup>, B. Guilhabert<sup>1</sup>, Q. Gao<sup>2</sup>, H.H. Tan<sup>2</sup>, C. Jagadish<sup>2</sup>, M.D. Dawson<sup>1</sup>

<sup>1</sup>Institute of Photonics, SUPA Dept. of Physics, University of Strathclyde, Technology and Innovation Centre, 99 George Street, G1 1RD, Glasgow, United Kingdom.

<sup>2</sup>Department of Electronic Materials Engineering, Research School of Physics and Engineering, The Australian National University, Canberra, ACT 2601, Australia

\*[antonio.hurtado@strath.ac.uk](mailto:antonio.hurtado@strath.ac.uk)

**Abstract:** We review our work on the accurate positioning of semiconductor nanowire lasers by means of nanoscale Transfer Printing (nano-TP). Using this hybrid nanofabrication technique, indium phosphide (InP) NWs are successfully integrated at selected locations onto heterogeneous surfaces with high positioning accuracy. Moreover, we show that NW lasers can also be organised to form bespoke spatial patterns, including 1- or 2-Dimensional arrays, or complex configurations with defined number of NWs and controlled separation between them. Besides, our nano-TP technique also permits the integration of NWs with different dimensions in a single system. Notably, the nano-TP fabrication protocols do not affect the optical or structural properties of the NWs and they retain their room-temperature lasing emission after their positioning onto all investigated receiving surfaces. This developed nano-TP technique offers therefore new exciting prospects for the fabrication of hybrid bespoke nanophotonic systems using NW lasers as building blocks.

## 1. Introduction

Nanowire photonics has emerged in recent years as a key-enabling field offering important advances across a wide range of scientific disciplines and applications. This span from energy generation, to bio-sensing, light-cell interfaces, nanophotonic integrated systems amongst others (see [1-3] and reference therein). Yet, all of these technological fields require novel systems and platforms allowing high-scale, versatile, flexible and cost effective device fabrication with low degradation and enhanced performance. Nanowire (NW) lasers fulfil all these conditions offering a revolution in photonics since they were first reported [4]. These provide highly localised coherent light emission and extremely reduced foot-print [1-4], features that ensure a key role for NW lasers in the next-generation nanophotonic integrated systems.

However, there are still key technological challenges for this to occur and for NW lasers to reach functional industrial products. One of these challenges, which directly arises from the ultra-small dimensions of NW lasers, make the manipulation and positioning of selected NWs at targeted locations on heterogeneous substrates with high precision and on industrial scales to produce functional systems a fundamental technological bottle-neck. This has limited greatly the transition of NW lasers from research laboratory environments into daily life products. Multiple techniques have been proposed for the manipulation of NWs. These include among others optical and optoelectronic tweezers [5], usage of microscope probes [6], large-scale printing techniques [7-11], and NWs' assembly mechanisms relying either on liquid-assisted [12], electric field [13] or Langmuir-Blodgett processes [14]. Nevertheless, these techniques have diverse difficulties and drawbacks, which might require complex expensive procedures or would only allow operation in fluid media (with NWs in solution). Furthermore, they would not permit the transfer of NWs across different

surfaces or the manipulation of single NWs. Other limiting aspects are the reduced positioning accuracy offered by some of the aforementioned techniques, or simply that they would not allow the integration of different types of NWs onto a single system. Moreover, no previous reports were found focusing on the accurate control and positioning of NWs with lasing emission at room temperature.

Recently, a technique known as transfer-printing (TP) [15] emerged from soft-lithography fabrication protocols. This uses elastometric polymer stamps to controllably pick-and-place optoelectronic structures, thus allowing transfer from their original substrate to a secondary receiving surface without damaging them or affecting their performance. This technique, first reported by Prof. Rogers' group at the University of Illinois in 2006 [15], has proven to be a very advantageous technique for hybrid optoelectronic device fabrication due to its simplicity and versatility to produce a myriad of hybrid systems. Soon after the first report of this technique, advances swiftly followed (for reviews see [9][16]) and different research groups have reported multiple hybrid photonic systems, based on TP processes. These included the systematic deposition of  $\mu$ -LEDs onto flexible substrates [17][18] and the integration of lasers on silicon platforms [16][19] just to name a few.

TP fabrication techniques have however mainly been centred on the manipulation of large-dimensional optoelectronic structures [16-19]. Although some effort focused at applying TP fabrication protocols to manipulate nanostructures, these have mainly dealt with large-printing approaches that did not permit the transfer printing of single nanoscale devices [7-11]. Also, to date the controllable integration of active NWs with lasing emission at room temperature had not been achieved, limiting the practical development of functional optical systems with these nanoscale and highly-localised laser sources.

At the Strathclyde's Institute of Photonics we have focused on this challenging technological aspect and

developed a new nanoscale TP (nano-TP) technique permitting successful operation at the extremely reduced scales of NW lasers [20][21]. Using our approach we demonstrate precise and sequential positioning of individual NWs with lasing emission at room temperature onto a variety of receiving substrates, such as polymers, metallic layers and silica [20][21]. Importantly our technique does not damage the NWs and they retained their lasing emission after the transfer printing processes. Moreover, by means of nano-TP we have built complex spatial arrangements with NW lasers, including 1- and 2-Dimensional arrays as well as arbitrary patterns with NWs with different properties whilst controlling also the number of NWs and the specific spacing between elements (down to just a few microns). Following these advances, our future plans include the use of the nano-TP technique for the hybrid fabrication of functional nanophotonic systems using NW lasers as building blocks.

The contents of this article are organized as follows: in Section 2 we describe the nano-TP technique. Sections 3 and 4 introduce respectively the NW lasers used in the nano-TP experiments and the  $\mu$ -Photoluminescence ( $\mu$ -PL) setup used to characterise their room temperature lasing emission. Section 5 includes experimental results on the precise positioning and organisation of NW lasers in multiple receiving surfaces and complex configurations by means of nano-TP protocols. Section 6 reports the conclusions and future plans for this research.

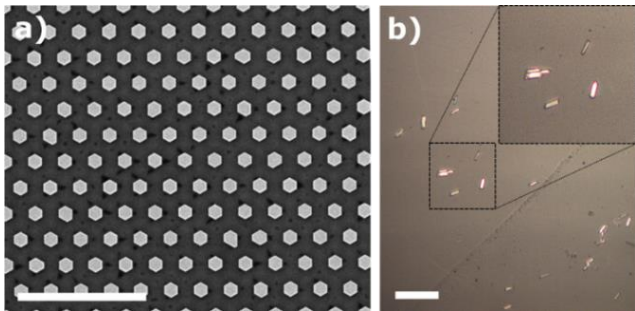


Fig. 1. InP NWs (a) as-grown and (b) after mechanical transfer to a 'donor' surface. Scale bars: (a) 4 $\mu$ m; (b) 30  $\mu$ m.

## 2. Semiconductor Nanowire Lasers

Semiconductor NWs are expected to be a key component across numerous applications, and one of the most investigated is their use as nanoscale laser sources (see [1-4][22-29] and references therein). Since the report of the first NW lasers over 15 years ago [4], research progress has been phenomenal, and NW lasers built from different materials, e.g. Group III-nitrides [22-24], Group II-VI [25], Group III-V [26-28], perovskites [29-31], and with operating wavelengths extending from the ultraviolet to the infrared have been demonstrated. The properties of NW lasers such as their highly localised emission and extremely reduced foot-print ensure that they will be key coherent light sources for nanophotonics-enabling technologies, e.g. as on-chip integrated photonic systems, optical interconnects, bio-sensors and light-cell probes [1-3].

For our work we have used indium phosphide (InP) NWs [27][28]. These had lasing emission at room temperature in the wavelength range of ~860-890 nm when subject to pulsed optical excitation. The InP NWs were grown by selective area metalorganic chemical vapour phase epitaxy

on InP substrates with patterned SiO<sub>2</sub> masks to control their dimensions. In our experiments we have used NWs of different sizes, with diameters ranging from 435 to 920 nm and lengths varying between 5 and 6  $\mu$ m. Fig. 1 shows an image of as-grown vertically-aligned InP NWs [28][29]. These were mechanically detached in bulk and randomly scattered on a 'donor' substrate (Si or SiO<sub>2</sub> typically) as shown in fig. 1(b), before carrying out the nano-TP protocols.

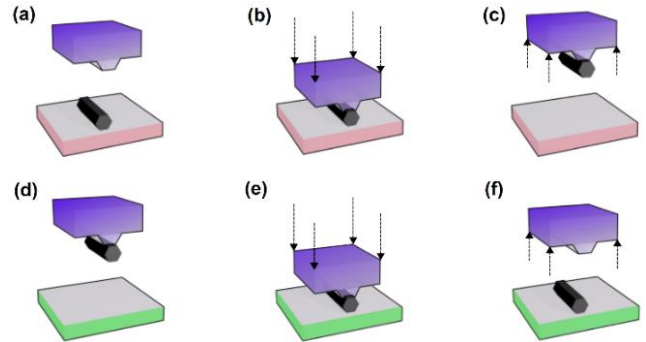


Fig. 2. Diagram of the various stages during the nano-TP process.

## 3. Nanoscale Transfer Printing

The nano-TP reviewed in this work uses a customized dip-pen lithography system permitting position control of a bespoke polymer  $\mu$ -stamp [20] with nanometer accuracy. The  $\mu$ -stamps were fabricated in polydimethylsiloxane, (PDMS) a transparent, elastomeric and adhesive polymer material. These properties permitted the use of these  $\mu$ -stamps to controllably capture an InP NW from the 'donor' substrate for its subsequent release at a targeted location on the 'receiver' substrate, whilst simultaneously permitting the imaging of the transfer printing process at all times. Notably, the developed nano-TP system also allowed operation across a total printing area of over 10 cm<sup>2</sup>. This enabled the 'donor' and 'receiver' substrates to be inches apart while retaining accurate positioning functionality in the order of tens of nanometers [18][20].

Fig. 2 shows a schematic diagram of the individual stages of the nano-TP of this work [20], as follows:

- (a) The  $\mu$ -stamp is aligned with a desired NW on the donor substrate.
- (b) Surface contact is produced between  $\mu$ -stamp and NW. The  $\mu$ -stamp deforms conforming to the NW's shape. The strong adhesion induced between NW and  $\mu$ -stamp allows the existing adhesion between substrate and NW to be overcome.
- (c) The  $\mu$ -stamp is lifted with the NW still adhering to it. The  $\mu$ -stamp relaxes to its original shape reducing its surface area in contact with the NW.
- (d) The  $\mu$ -stamp is moved and aligned to a targeted location on the receiver substrate.
- (e) Surface contact is produced between the system formed by the  $\mu$ -stamp with the captured NW and the receiver substrate. Gentle mechanical pressure is applied until the adhesion between surface and NW is enough to overcome that between NW and  $\mu$ -stamp.
- (f) The  $\mu$ -stamp is lifted away leaving the NW printed at the targeted position on the receiver substrate.

We have designed and fabricated two different types of  $\mu$ -stamps. These were fabricated in PDMS with equal

dimensions ( $30 \times 10 \mu\text{m}$  rectangular mesas and  $50 \mu\text{m}$  height), but different tips, the actual part of the stamp used to capture and release the NWs. The first generation of  $\mu$ -stamps had a flat tip, whilst the second generation of  $\mu$ -stamps was fabricated with a V-shape tip. Fig. 3 depicts the structures of the  $\mu$ -stamps used in the work. Fig. 3(a) shows a lateral view image of a V-shape tip  $\mu$ -stamp, whilst fig. 3(b) shows the top view of a  $\mu$ -stamp with its body in cream colour and the  $\mu$ -tip in black at the centre. Schematics (i) and (ii) in fig. 3(b) show respectively the shape for the V-shape and flat tip  $\mu$ -stamps. Both types of  $\mu$ -stamps demonstrated their ability to transfer-print NW lasers from their ‘donor’ to heterogeneous receiving surfaces. However, given their distinct structures, they offered different performance. The first generation of flat-tip  $\mu$ -stamps provided a bigger contact surface between  $\mu$ -stamp and NW which enabled the adhesion between NW and ‘donor’ substrate to be overcome easily thus allowing an easier capture of the NW. However, precisely because of the high adhesion between NW and  $\mu$ -stamp, they delivered a more difficult NW release procedure. These first type of  $\mu$ -stamps were therefore adopted for the transfer-printing of NWs from the donor substrate to adhesive surfaces such as PDMS, but were less suitable for the transfer of NWs onto less adhesive substrates such as metals. The second generation of V-shape  $\mu$ -stamps were designed to resolve this issue. The lateral view image of a V-shape  $\mu$ -stamp (see fig. 3(a)) clearly depicts its characteristic of a ‘pointy’ tip. The latter provided a reduced contact surface between the NW and  $\mu$ -stamp, as compared with their flat tip counterparts. However, this design still allowed successful NW capture from the donor substrate, whilst facilitating the NW release process by making it easier to overcome the adhesion between NW and  $\mu$ -stamp in the printing phase on the receiving substrate. This enhanced the yield of the technique when operating with non-adhesive receiving substrates such as silica or gold.

Notably, the structure of the  $\mu$ -stamps did not suffer changes during the nano-TP processes, thus permitting their reutilisation for the sequential transfer-printing of multiple NWs to either form bespoke spatial arrangements or for their integration onto different substrates. An additional important consideration regarding the  $\mu$ -stamp fabrication refers to its adherence characteristics. The use of adhesive stamps indeed permitted the capture of NWs from their ‘donor’ substrate. Hence, the  $\mu$ -stamps were designed in PDMS with a selected PDMS/potting agent composition of 10:1 which made them ‘sticky’ to permit the capture of NWs from the ‘donor’ substrate. Finally, the deformation of the  $\mu$ -stamp’s shape around the NW during capture was an important feature of the technique. This could be investigated visually during the nano-TP processes, thanks to the optical imaging system included in the nano-TP’s system configuration.

To fabricate the  $\mu$ -stamps, micrometric Silicon (*Si*) molds with a negative pattern of the designed  $\mu$ -stamp were produced. These patterns were made using the crystallographic etching planes of *Si* along with high aspect ratio SU-8 structures. A selected *Si* mold was then placed on a petri dish before liquid and degassed PDMS was poured into it. This was left to harden 24 hours at room temperature, before being placed on a hot-plate for 2 hours at  $100^\circ\text{C}$ . Finally, the PDMS material with the patterned  $\mu$ -stamp was peeled off the *Si* mold and cut to a suitable size for operation in our nano-TP system. Prior to that, the  $\mu$ -stamp was tested

to verify that it had a uniform height across its structure. This was done to avoid poor performance arising from unwanted tilts in the  $\mu$ -stamp providing different surface contact with the donor/receiving substrates across the stamp.

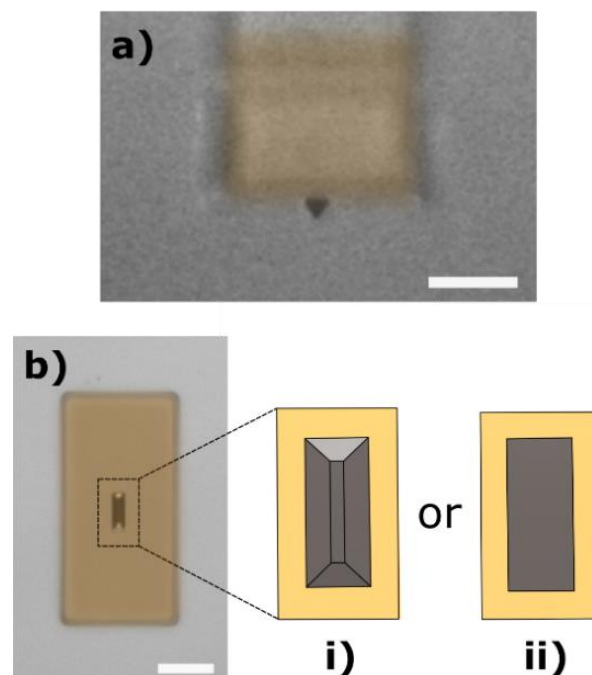


**Fig. 3.** (a) Lateral and (b) top image of a V-shape tip  $\mu$ -stamp. Schematic of the two types of  $\mu$ -stamps with (i) flat- and (ii) V-shape tip are also included in (b). Scale bars  $50 \mu\text{m}$ .

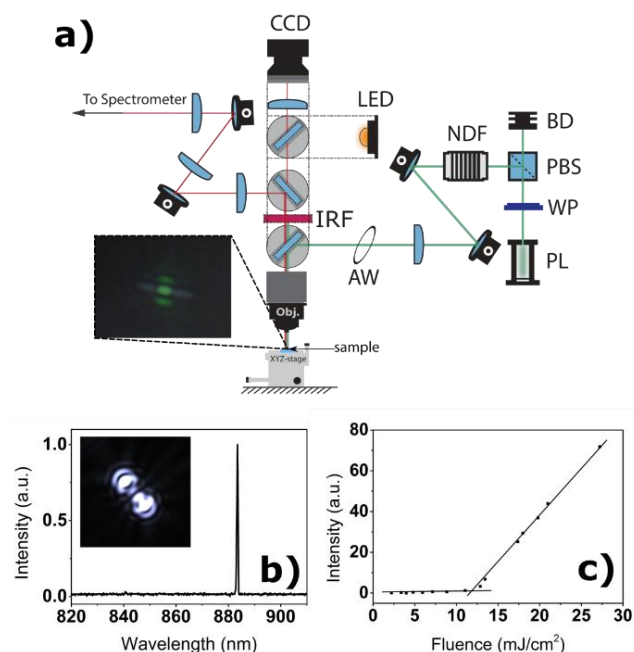


**Fig. 4.** (a)  $\mu$ -PL setup used in this work. (b) Micrograph, spectrum and (c) lasing threshold curve of an InP NW.

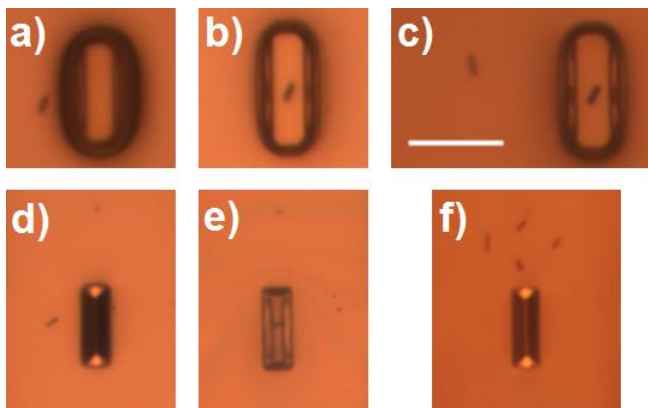
#### 4. Characterisation Setup

Fig. 4(a) shows the  $\mu$ -photoluminescence ( $\mu$ -PL) setup used in this work to characterise the room-temperature lasing emission from the InP NWs. This setup was used before and after carrying out the nano-TP processes to check that the NWs retained their lasing emission after their positioning at different locations onto heterogeneous substrates. A 532 nm

frequency-doubled Nd:YAG pulsed solid-state laser, emitting 1.6 ns long pulses with a repetition rate of 10 kHz, was used to optically excite the InP NWs above their lasing threshold. This specially designed  $\mu$ -PL setup permitted the optical pumping of NWs whilst simultaneously collecting their lasing emission through a high-resolution spectrometer incorporated with a CCD camera. Full details on the characterisation setup can be found in [20]. Fig. 4 shows a captured image and the measured optical spectrum for a lasing InP NW (435nm diameter) showing clearly light emission from its end-facets and yielding a narrow spectral peak when optically excited above its lasing threshold.

## 5. Results

Our first goals were to demonstrate the achievement of precise and repeatable positioning of NW lasers onto a wide variety of substrates of interest for photonics systems, such as PDMS, silica and gold. Initially, we used our first generation of flat-tip  $\mu$ -stamps and focused on the transfer-printing of NW lasers onto PDMS receiving substrates. PDMS was initially chosen because it is a very adherent material thus allowing an easier NW releasing process by providing a stronger bond between NW and receiver substrate. This resulted in a more accessible route towards the achievement and demonstration of accurate transfer printing of NW lasers. Additionally, integration of NW lasers onto flexible transparent substrates is of interest for the future development of flexible integrated nanophotonic systems with NW lasers at their core.



**Fig. 5.** Images showing the transfer printing of NW lasers from a Si substrate to PDMS (a-c) and silica (d-f) surfaces using respectively a flat- (a-c) and V-shape (d-f)  $\mu$ -stamp. Scale bar 30  $\mu$ m. Adapted with permission from [20].

Figs. 5(a-c) show sequential images of the transfer printing of an InP NW laser from its ‘donor’ (Si) substrate to a selected location on a PDMS surface using a flat-tip  $\mu$ -stamp. Fig. 5(a) shows the  $\mu$ -stamp aligned next to a selected NW lying down on the donor (Si) surface. Fig. 5(b) shows the NW captured by the  $\mu$ -stamp while fig. 5(c) depicts the  $\mu$ -stamp with the captured NW about to be printed on the receiving PDMS surface at a selected location next to a previously printed NW. It should be noted that all the images included in fig. 5 were directly obtained using the optical system integrated in our nano-TP setup through the transparent PDMS  $\mu$ -stamps.

After this initial demonstration of the feasibility of this technique to controllably transfer-print NW lasers onto a PDMS surface, we investigated transfer-printing of NWs onto other less adhesive substrates. For that, we used our V-

shaped tip  $\mu$ -stamps (see fig. 3). As previously stated, these tips offered a reduced surface contact between  $\mu$ -stamp and NW, thus allowing an easier route for NW release on the receiving substrate whilst still enabling NW capture from the donor surface. Fig. 5(d-f) shows sequential images illustrating the successful transfer printing of a NW laser from a donor Si substrate to a Silica surface using a V-shape  $\mu$ -stamp. Fig. 5(d) shows the  $\mu$ -stamp aligned next to the selected NW on the donor substrate. Now the tip of the NW can be seen in black as a result of its sloped sides (see fig. 3(a)) whilst the  $\mu$ -stamp’s central sub-micrometric ridge can be seen as a faint transparent line at the centre of the stamp. Fig. 5(e) shows the stamp as it captures the NW from the donor substrate. Fig. 5(e) also shows clearly the deformation of the  $\mu$ -stamp’s tip as pressure is applied to ensure the NW is captured. Also as a result of this deformation the  $\mu$ -stamp becomes flatter and therefore transparent as it conforms to the NW’s structure. Upon capturing the NW and lifting the  $\mu$ -stamp away from the donor substrate, its structure relaxes to its original V-shape reducing its contact surface with the NW, enabling therefore an easier NW release in the silica receiving substrate. Finally, fig. 5(f) depicts the  $\mu$ -stamp after releasing the NW (located right above it) on the silica surface next to other three previously printed NWs to form a basic closed-loop pattern. It should be mentioned that the nano-TP technique allows positioning of a NW with micrometer accuracy. This can be seen in fig. 5(f) where a 4 NWs are separated by only just a few microns. In addition to the results shown in fig. 5 for PDMS and silica substrates, we have also demonstrated that this technique can also be used to precisely transfer NW lasers onto a wide variety of surfaces [20]. We must note that our main goal during this work, was to tackle an important technological challenge, namely the accurate positioning of individual NW lasers onto different surfaces/systems. This is of importance for the future manufacturing of hybrid and bespoke nanophotonic systems with integrated NW laser sources. Hence, our  $\mu$ -stamps used during the nano-TP processes were designed with relatively small cross-section (30 x 10  $\mu$ m) to permit single device capture. However, we should also indicate that our technique would also permit the transfer-printing of multiple nanoscale devices at once by using stamps with larger cross-sectional areas.

Our next focus was to demonstrate the possibility to build complex spatial arrangements with different types of NW lasers onto a variety of platforms by means of nano-TP. Fig. 6 shows various regular 2D arrays fabricated with InP NW lasers as building blocks using nano-TP. Specifically, fig. 6 shows two arrays with alternating (fig. 6(a)) or aligned rows (fig. 6(b)) fabricated on a PDMS receiving substrate. Moreover, the spacing between the individual elements in the array could be controlled and made equal to  $\sim$ 25  $\mu$ m for the results in fig. 6).

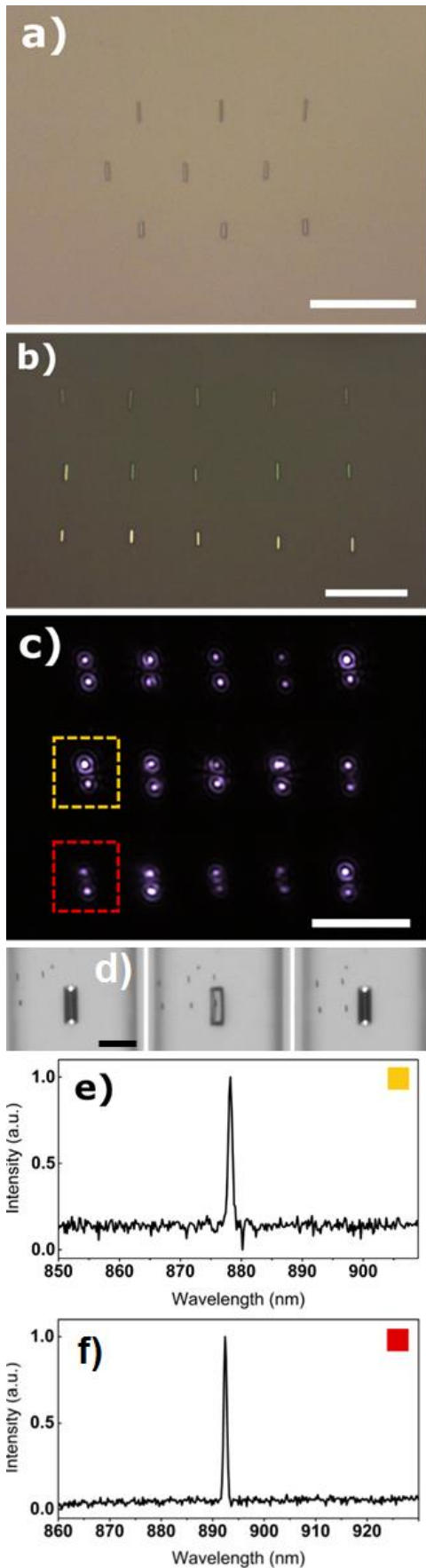


**Fig. 6.** 2-D arrays fabricated with InP NW lasers by means of nano-TP on a PDMS substrate with (a) alternating and (b) aligned rows. (c) Collage merging images for the lasing NWs in (b). (d) Sequential images illustrating the printing of one of the NWs in the array in (b). (e & f) Spectra for the indicated NW lasers in the array in (b). Scale bars: (a & b) 30  $\mu\text{m}$ ; (c) 20  $\mu\text{m}$  and (d) 30  $\mu\text{m}$ .

Additionally, fig. 6 also shows that different types of NW lasers could be integrated into a single array. For both arrays plotted in Figs. 6(a) and 6(b), the top row was solely composed by 435 nm diameter NWs, whilst the middle and bottom rows were formed by NWs with 660 and 920 nm diameters, respectively. Moreover, the NWs exhibited lasing emission from their end-facets after their integration at the desired locations in the arrays on the PDMS substrates. This is shown in fig. 6(c) which plots a collage merging individually captured micrographs of all NWs in the array included in fig. 6(b) when optically excited above their lasing thresholds. Fig. 6, therefore shows that our nano-TP technique permits the formation of nanolaser arrays with flexible and bespoke spatial designs which can be engineered at will depending on the specific targeted applications and which not rely in fixed device structures [32]. Fig. 6(d) illustrates the process of fabricating the array in fig. 6(b) by means of nano-TP protocols. Specifically, fig. 6(d) shows sequential images depicting the alignment of the  $\mu$ -stamp with a captured NW at the desired position in the array (left plot), surface contact between  $\mu$ -stamp and substrate for NW release (middle plot) and the printed NW at the desired location in the array with the  $\mu$ -stamp next to it (right plot). Finally, figs. 6(e) and 6(f) show the lasing spectrum from two selected InP NW lasers after their integration in the array in fig. 6(b). Specifically, figs. 6(e) and 6(f) show respectively measured spectra for the 660 and 920 nm diameter NWs marked by the yellow and red dashed squares in fig. 6(b). Moreover, the individual NWs in the arrays in fig. 6 have different dimensions and thus distinct emission wavelengths (see figs. 6(e) and 6(f)) which opens the door for future multi-wavelength grids of NW lasers on diverse selected surfaces.

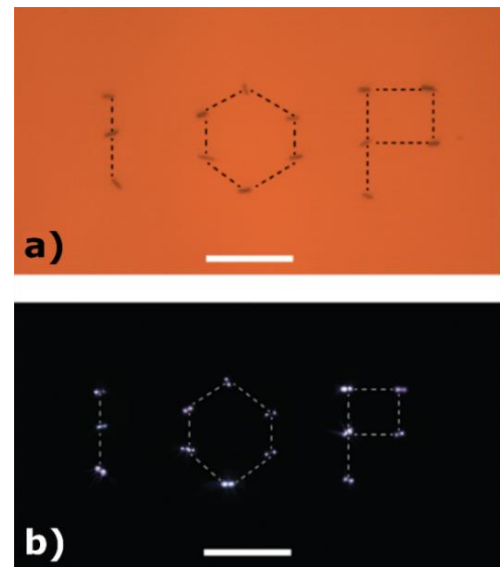


**Fig. 7.** 'IOP' acronym built with InP NW lasers (435 nm diameter) on a PDMS surface. (a) Image of the pattern captured with the optical system of the nano-TP setup (b) collage of the lasing NWs in the pattern. Scale bars 50  $\mu\text{m}$ . Adapted with permission from [20].

To better showcase the flexibility and possibilities of our nano-TP technique, we have also used it to produce bespoke complex spatial patterns with InP NW lasers. The example included in fig. 7 illustrates the formation of the acronym 'IOP', initials of the Strathclyde's Institute of Photonics with 435 nm diameter NWs controllably separated by just a few tens of microns. To help the reader, dashed lines

joining the individual NWs in the pattern are included in the two plots depicted in fig. 7. Fig. 7(a) shows a CCD image of the ‘IOP’ patterns which was built on a PDMS receiving substrate. Fig. 7(b) plots a collage combining the micrographs of each NW lasing upon excitation with a pump laser.

## 6. Conclusion

We review our recent work on the newly developed nanoscale transfer printing technique (or nano-TP). Using this hybrid nanofabrication method we demonstrate the precise manipulation, organisation and positioning of semiconductor NW lasers onto different surfaces widely used in photonic technologies. Our results to date have shown that it is indeed possible to integrate InP NW lasers with different dimensions (with diameters ranging from 435 to 920 nm) onto polymer (PDMS), silica, silicon and metallic (gold) surfaces with sub-micrometer positioning accuracy. Our nano-TP technique relies on bespoke polymer elastomeric  $\mu$ -stamps which enable the controllable capture and release of NW lasers; therefore allowing their transfer from a primary (or ‘donor’) substrate onto a targeted surface with very high positioning accuracy. Notably, the InP NW lasers retained their room-temperature lasing emission (without any significant changes in lasing threshold or linewidth) and structural properties after the transfer-printing processes in all the ‘receiving’ substrates investigated. Until now, our research has exclusively focused on the manipulation of InP NW lasers with emission in the infrared range of the spectrum. Yet we believe that this technique can also be extended to other NW lasers and other types of semiconductor nanostructures built from different material systems, with diverse structures and dimensions and with light emission at different wavelengths. Our nano-TP technique permits the feasible fabrication of complex spatial patterns, such as 1D/2D and other micrometric bespoke configurations, using NW lasers as building blocks. Moreover, we show that our nano-TP technique also allows the integration of devices with distinct features (e.g. different dimensions) to form a certain spatial pattern. In summary, our recently developed nano-TP technique provides a simple, versatile and flexible approach for the precise fabrication of bespoke nanophotonic systems using NW lasers as the building block, benefitting from the unique features of these ultra-small laser sources and impacting numerous applications. These may expand from photonic integrated systems for on-chip functionalities to highly-localised light sensing modules among many others.

## 7. Acknowledgments

Financial support for this work was provided by the University of Strathclyde (through the Strathclyde’s Chancellor Fellowship Program), the Australian Research Council, and the UK’s Engineering and Physical Sciences Research Council (grant EP/I029141/1). We thank the Australian National Fabrication Facility, ACT Node, for access to the growth facilities used in this work.

## 8. References

- (1) Yan, R.; Gargas, D.; Yang, P., *Nat. Photon.* **2009**, 3, 569-576.
- (2) Yang, P.; Yan, R.; Fardy, M., *Nano Letts.* **2010**, 10, 1529-1536.
- (3) Eaton, S.W., Fu, A., Wong, A.B., Ning, C.-Z. and Yang, P., *Nat. Rev. Mat.* **2016**, 1, 16028.
- (4) Huang, M.H.; Mao, S.; Feick, H.; Yan, H.; Wu, Y.; Kind, H.; Weber, E.; Russo, R.; P. Yang., *Science* **2001**, 292, 1897-1899.
- (5) Pauzauskie, P.J., Radenovic, A., Trepagnier, E., Shroff, H., Yang, P., Liphardt, J., *Nat. Materials* **2006**, 5, 97–101.
- (6) Xu, H.; Hurtado, A.; Wright, J.B.; Li, C.; Liu, S.; Figiel, J.J.; Luk, T.-S.; Brueck, S.R.J.; Brener, I.; Balakrishnan, G.; Li, Q.; Wang G.T., *Opt. Exp.* **2014**, 22, 19198-19203.
- (7) Lee, C.H.; Kim, D.R.; Zheng, X., *PNAS* **2010**, 107, 9950-9955.
- (8) Ahn, J.-H.; Kim, H.-S.; Lee, K.-J.; Jeong, S.; Kang, S.J.; Sun, Y.; Nuzzo, R.G.; Rogers, J.A., *Science* **2006**, 314, 1754.
- (9) Carlson, A.; Bowen, A.M.; Huang, Y.; Nuzzo, R.G.; Rogers, J.A., *Adv. Mater.* **2012**, 24, 5284-5318.
- (10) Javey, A.; Nam, S.; Friedman, R.S.; Yan, H.; Lieber, C.M., *Nano Letts.* **2007**, 7, 773-777.
- (11) Fan, Z.; Ho, J.C.; Jacobson, Z.A.; Yerushalmi, R.; Alley, R.L.; Razavi, H.; Javey, A., *Nano Letts.* **2008**, 8, 20-25.
- (12) Huang, Y.; Duan, X.; Wei, Q.; Lieber, C. M. *Science* **2001**, 291, 630-633.
- (13) Duan, X.; Huang, Y.; Cui, Y.; Wangm J.; Lieber, C.M., **2001**, *Nature* 409, 66-69.
- (14) Jin, S.; Whang, D.; McAlpine, M.C.; Friedman, R.S.; Wu, Y.; Lieber, C.M.; *Nano Letts.* **2004**, 4, 915-919.
- (15) Meitl, M.A.; Zhu, Z.T.; Kumar, V.; Lee, K.J.; Feng, X.; Huang, Y.Y.; Adesida, I.; Nuzzon, R.G.; Rogers, J.A., *Nat. Mater.* **2006**, 5, 33-38.
- (16) Corbett, B., Loi, R., Zhou, W., Liu, D., Ma, Z., *Prog. Quantum Electron.*, **2017**, 52, 1-17
- (17) Carlson, A.; Bowen, A.M.; Huang, Y.; Nuzzo, R.G.; Rogers, J.A., *Adv. Mater.* **2012**, 24, 5284-5318.
- (18) Trindade, A.J.; Guilhabert, B.; Massoubre, D.; Zhu, D.; Laurand, N.; Gu, E.; Watson, I.M.; Humphreys, C.J.; Dawson, M. D., *Appl. Phys. Letts.* **2013**, 103, 253302.
- (19) Sheng, X.; Robert, C.; Wang, S.; Pakeltis, G.; Corbett, B.; Rogers, J.A., *Laser & Phot. Rev.* **2015**, 9, L17-L22.
- (20) Guilhabert, B., Hurtado, A., Jevtics, D., Gao, Q., Tan, H.H., Jagadish, C., *ACS Nano*, **2016**, 10, 3951-3958.
- (21) Hurtado, A., Jevtics, D., Guilhabert, B., Gao, Q., Tan, H.H., Jagadish, C. and Dawson, M.D., *SPIE Newsroom Lasers & Sources*, **2017**, 1-3, DOI: 10.1117/2.1201612.006830
- (22) Johnson, J.C.; Choi, H.-J.; Knutsen, K.P.; Schaller, R.D.; Yang, P.; Saykally, R.J., *Nat. Mater.* **2002**, 1, 106-110.
- (23) Gradecak, S.; Qian, F.; Li, Y.; Park, H.-G.; Lieber, C.M., *Appl. Phys. Letts.* **2005**, 87, 173111.
- (24) Li, Q.; Wright, J.B.; Chow, W.W.; Luk, T.S.; Brener, I.; Lester, L.F.; Wang, G.T., *Opt. Exp.* **2012**, 20, 17873-17879.
- (25) Zimmler, M.A.; Capasso, F.; Muller, S.; Ronning, C., *Semicond. Sci. Technol.* **2010**, 25, 024001.
- (26) Chen, R.; Tran, T.D.; Ng, K.W.; Ko, W.S.; Chuang, L.C.; Sedgwick, F.G.; Chang-Hasnain, C.; *Nat. Photon.* **2011**, 5, 170-175.
- (27) Gao, Q.; Saxena, D.; Wang, F.; Fu, L.; Mokkaapati, S.; Guo, Y.; Li, L.; Wong-Leung, J.; Caroff, P.; Tan, H.H.; Jagadish, C., *Nano Letts.* **2014**, 14, 5206-5211.
- (28) Saxena, D.; Wang, F.; Gao, Q.; Mokkaapati, S.; Tan, H.H.; Jagadish, C., *Nano Letts.* **2015**, 15, 5342-5348.
- (29) Zhu, H., Fu, Y., Meng, F., Wu, X., Gong, Z., Ding, Q., Gustafsson, M.V., Trinh, M.T., Jin, S. and Zhu, X.Y., *Nat. Mat.*, **2015**, 636-642.
- (30) Eaton, S.W., Lai, M., Gibson, N.A., Wong, A.B., Dow, L., Ma, J., Wang, L.-W., Leone, S.R. and Yang, P., *PNAS*, **2016**, 113, 1993-1998
- (31) Zhou, H., Yuan, S., Wang, X, Tao, X., Wang, X., Li, H., Zheng, W., Fan, P., Li, Y., Sun, L., and Pan, A., *ACS Nano*, **2017**, 11, 1189-1195.
- (32) Zhang, Q., Zhu, X., Li, Y., Liang, J., Chen, T., Fan, P., Zhou, H., Hu, W., Zhuang, X., and Pan, A., *Las. & Photon. Rev.*, **2016**, 10, 458-464.